PERFORMANCE CHARACTERISTICS OF A GRASSED-WATERWAY TRANSITION

ARS-S-158

February 1977

AGRICULTURAL RESEARCH SERVICE • U.S. DEPARTMENT OF AGRICULTURE

Agricultural Research Service
UNITED STATES DEPARTMENT OF AGRICULTURE
in cooperation with
Oklahoma Agricultural Experiment Station

CONTENTS

ILLUSTRATIONS

TABLES

PERFORMANCE CHARACTERISTICS OF A GRASSED-WATERWAY TRANSITION

By W. O. Ree[1]

ABSTRACT

This report describes the performance of a channel transition at the end of a grassed waterway during 11 test flows ranging from 0.83 to 145 ft^3/s to determine the ability of the transition to reduce velocity from supercritical to subcritical without erosion. The transition performed admirably and suffered no erosion or cover loss from the flows. This good performance is attributed to a design that incorporates a gradual convergence of the conjugate depths, thus limiting hydraulic jump to a nondestructive minimum. Maintaining a dense, uniform bermudagrass cover also contributed to the success of the transition. **KEYWORDS: channel design, erosion control, grassed-waterway transition, test flows.**

INTRODUCTION

A grassed waterway at the Water Conservation Structures Laboratory conveys flows from the main supply canal to the bottom land below (fig. 1). A portion of the waterway is on a steep slope, where velocities for the larger flows become supercritical. The flows are discharged onto a bottom area of zero slope. A carefully shaped reach between the steep channel and the bottom area provides the transition for these flows to the bottom. The flows are discharged into the waterway before and after each test on the adjacent experimental channels. Thus, the waterway receives intensive use during a busy testing season.

When the transition was being planned, the laboratory was already under construction, and the designers (who were also the builders) did not have the time to study transition design. So they designed the geometry of the transition (fig. 2) to change the cross section and slope

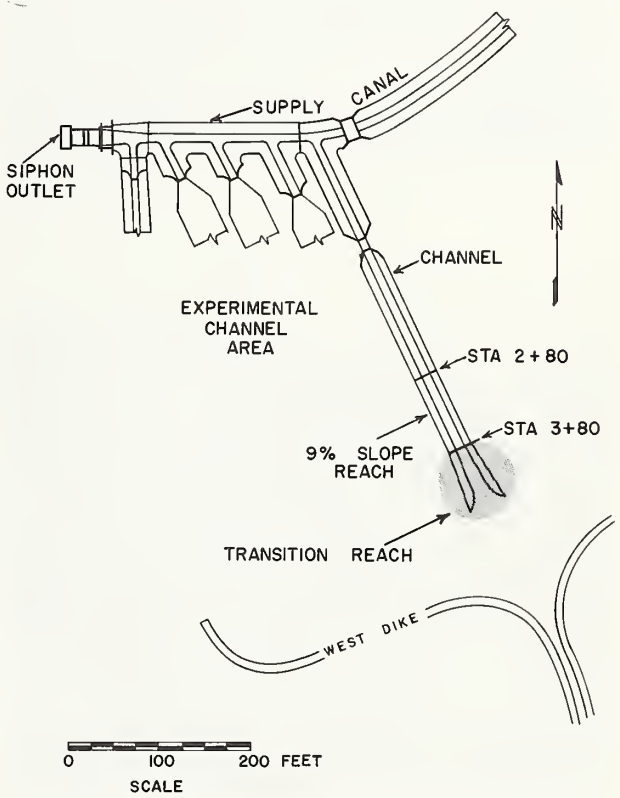

FIGURE 1.—Experimental channel area, including grassed waterway with transition.

[1] Research leader, Water Conservation Structures Laboratory, Agricultural Research Service, U.S. Department of Agriculture, Stillwater, Okla. 74074 (retired).

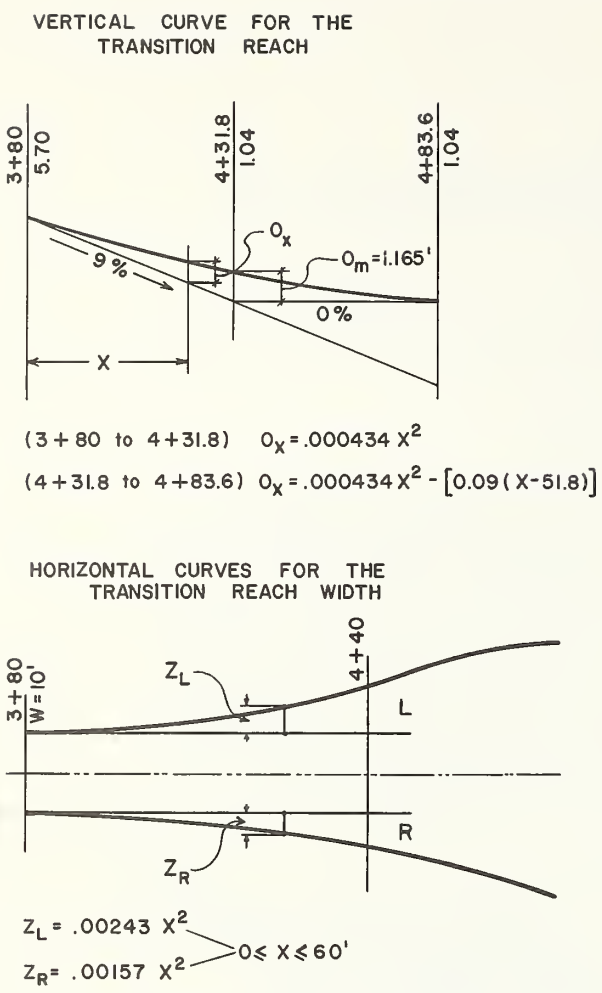

FIGURE 2.—Geometry of transition.

of the channel to be as gradual as possible in the space provided. A test channel to the right and a road to the left limited freedom of choice, and the asymmetric plan allowed the greatest widening of the channel.

Because of the uncertainties of the intuitive and empirical nature of the design, there was some uneasiness about the probable performance of the transition. The designers envisioned the possibility of a hydraulic jump and accompanying deep erosion of the transition bed during flow, but when the completed transition conveyed the maximum flow without erosion damage, the designers were immediately put at ease. After about 10 more such flows were safely conveyed, controlled tests were run on the transition to establish the reasons for its successful operation. These tests disclosed why a hydraulic jump was not evident and also provided data on hydraulic resistance in an expanding channel. Some design principles were deduced from these tests and are presented in this report, together with a description of the transition and the tests.

TRANSITION

Design

The transition begins at station 3+80, the lower end of a trapezoidal channel having a bottom width of 10 ft and side slopes of 4 to 1. The bottom slope of the channel for the 100 ft immediately upstream of station 3+80 is 9 percent. When the transition was being designed, there was concern over the possible effects of a hydraulic jump on the stability of the transition because its only protection was to be a bermudagrass lining. So the channel was flared gradually to increase its width, and a vertical curve was introduced to change the bottom slope from 9 to zero percent (fig. 2). It was hoped that these changes would reduce channel-exit flow velocity and reduce or eliminate a hydraulic jump at the exit. Parabolic curves were used for both gradient decrease and width increase.

The bottom width of the transition is

$$W = 10 + Z_L + Z_R,$$

where $Z_L = 0.00243X^2$,
and $Z_R = 0.00157X^2$,
and where W = transition width (feet),
Z = distance from toe of channel side to line of straight-channel toe line extended (feet),
X = distance from station 3+80, the start of transition (feet), but not to exceed 4+40 ($0 \leq X \leq 60$ ft),
L = subscript denoting left side of transition, facing downstream,
and R = subscript denoting right side of transition, facing downstream.

The rates of divergence for the two sides of the channel are as follows:

For the left side, $\frac{dZ_L}{dX} = 0.00486X$.

For the right side, $\frac{dZ_R}{dX} = 0.00314X$.

The transition depth contours, as-built profile, and cross sections are shown in figure 3.

Vegetation

The lining for the transition was an excellent stand of very uniformly distributed bermudagrass. Figures 4 and 5 show the transition before the tests. At that time the cover was green and unmowed, with an average length of 6.7 in. The grass lengths and stand counts were measured at selected points on the cross section of each 10-ft station (table 1).

TABLE 1.—*Stand counts and average stem lengths for bermudagrass in transition*

Profile station (ft)	Cross section station[1] (ft)	Stand count (stems/ft^2)	Average stem length (in)
3+80	2L	328	4.5
3+90	2R	472	5.5
4+00	0	416	6.0
4+10	6L	448	8.5
4+20	8R	388	8.0
4+30	3R	468	5.5
4+40	16L	428	9.0
4+50	16R	412	8.5
4+60	10L	456	6.0
4+70	10R	404	6.0
4+80	6L	456	6.0
Average	...	425	6.7

[1] L, left side of channel. R, right side of channel.

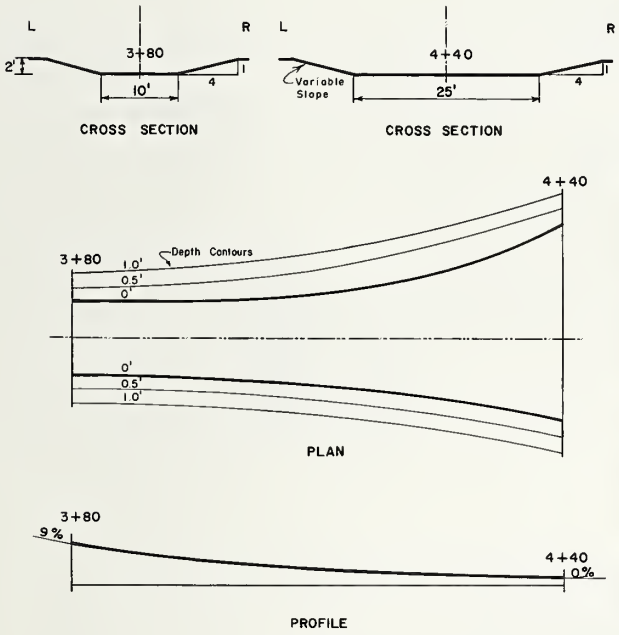

FIGURE 3.—Profile, plan, and cross sections of transition.

Determining the average length and number of bermudagrass stems per unit area is a difficult task beset with uncertainties, one of which is stem-length definition. Bermudagrass is stoloniferous, with "runners" extending out from the parent plant. Wherever a node touches the ground, rooting will occur, and a new plant will start sending stems upward and stolons outward. Stem length is measured from the rooting point to the tip of the stretched out stem, but stolons are not generally measured. However, short, unrooted stolons may be indistinguishable from stems and may or may

FIGURE 4.—Transition before tests, as viewed from upstream.

FIGURE 5.—Transition before tests, as viewed from downstream.

not be measured, depending upon the observer. The stems may be branched, but this poses no problem when measuring length because only the longest stems are measured. The branching does present a vexing problem when counting the number of stems per unit area. Generally, the minor (shorter) branches are ignored, and the longer, predominant branches may be counted as separate stems. So there is a strong subjective element in stand-count and stem-length determinations. However, within the group of observers at the laboratory, techniques tend to become uniform, and stand-count and stem-length data are fairly consistent.

A stand count of 425 stems/ft^2 is a good cover. This cover quality and the average stem length of 6.7 inches place the channel lining in the class C retardance category. See the "Handbook of Channel Design for Soil and Water Conservation"[2] for retardance class descriptions.

TEST PROCEDURES

Before the tests were begun, cross sections were measured at 10-ft intervals along the transition, starting with station 3+80 and continuing for 110 ft. Ground elevations were measured with an engineer's level and rod to the nearest 0.01 ft at 1-ft intervals across the channel.

Eleven test flows, ranging from 0.83 to 145 ft^3/s, were discharged through the transition in order of increasing magnitude. During each test flow (lasting about 1 hour), water-surface elevations at the right and left edges of each 10-ft station were determined with an engineer's level and rod. Measurements were limited to these two locations because they were the only accessible points. Bridges to span the channel were not available, and wading would have disturbed the flow and probably would have drenched the rod man. Studies of data from tests on a similar channel, in which water-surface elevations were determined at 1-ft intervals across the station, indicated that the maximum error in computing the Manning n value (using only the two edge elevations) would be to increase n by less than 4 percent. Also, the distance of the water's edge from the channel centerline was determined for each side. Having the edge-of-water locations eliminated the need to plot cross sections and permitted the direct computation of the cross-sectional area and the wetted perimeter.

The discharge rates for the first four tests were measured with a 1.5-ft H-flume installed at the head of the test channel. For the seven larger flows the discharge rates were measured

[2] U.S. Dep. Agric., Soil Conserv. Serv. [Rep.] SCS–TP–61, 34 pp. (1954).

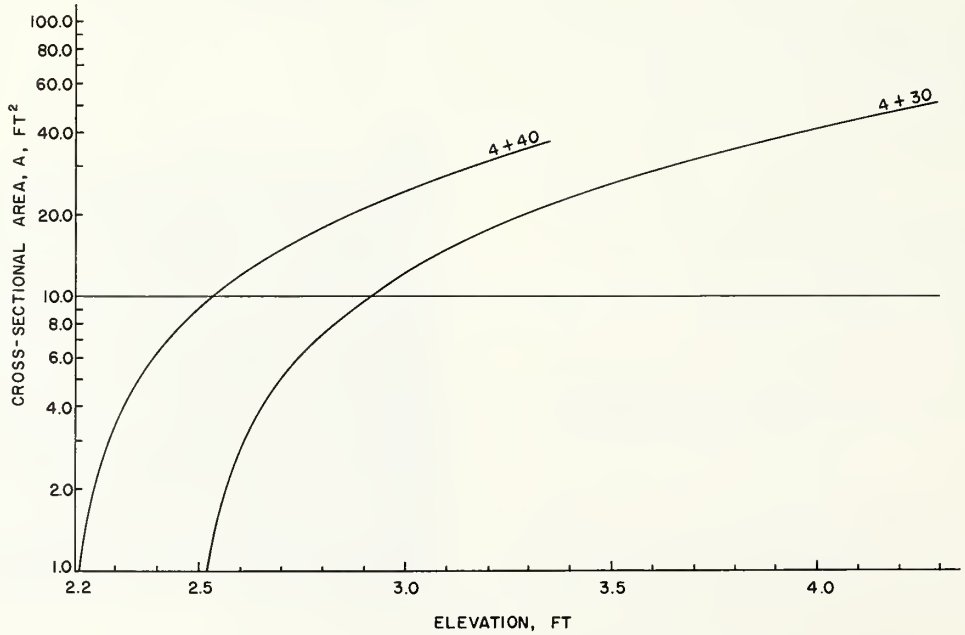

FIGURE 6.—Area-elevation curves for stations 4+30 and 4+40.

with the main weir at the head of the supply canal. Estimated leakage between the weir and the test channel was deducted from the weir measurement. The accuracy of the discharge measurements is estimated to be ±5 percent.

CALCULATIONS

The average water-surface elevations for each test were calculated for each 10-ft station in the transition. Station cross-sectional areas and wetted perimeters were calculated for each of these water-surface elevations. Additional cross-sectional areas were calculated for water-surface elevations (either above or below the test elevations) for later use in calculating conjugate depths. The areas were plotted against the elevations to facilitate this use; a typical plotting is shown in figure 6.

Manning *n* Values

Manning *n* values were calculated for each test for each 10-ft subreach by solving the Manning formula.

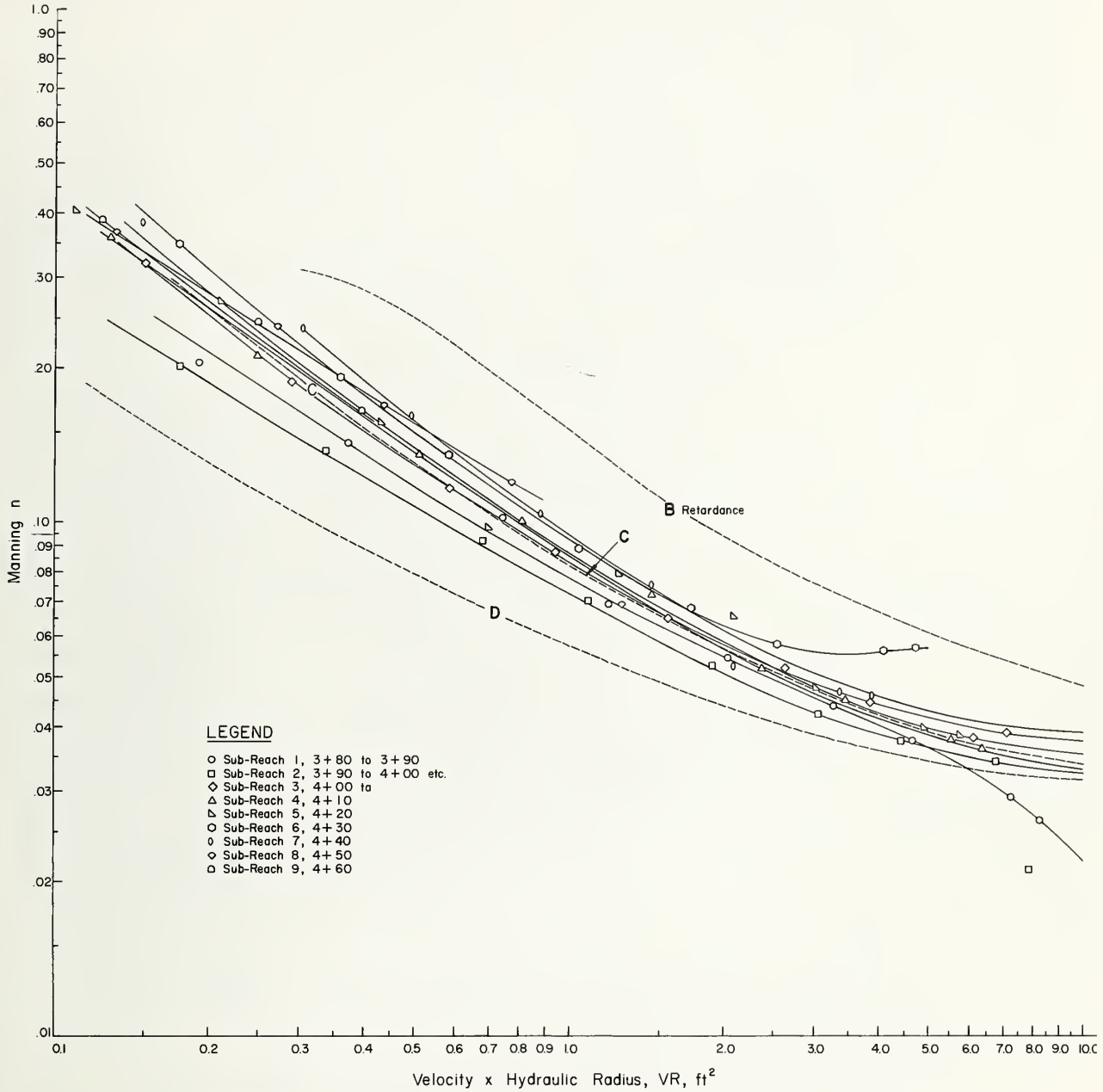

FIGURE 7.—Manning *n* versus product of velocity and hydraulic radius (*VR*) for subreaches in transition.

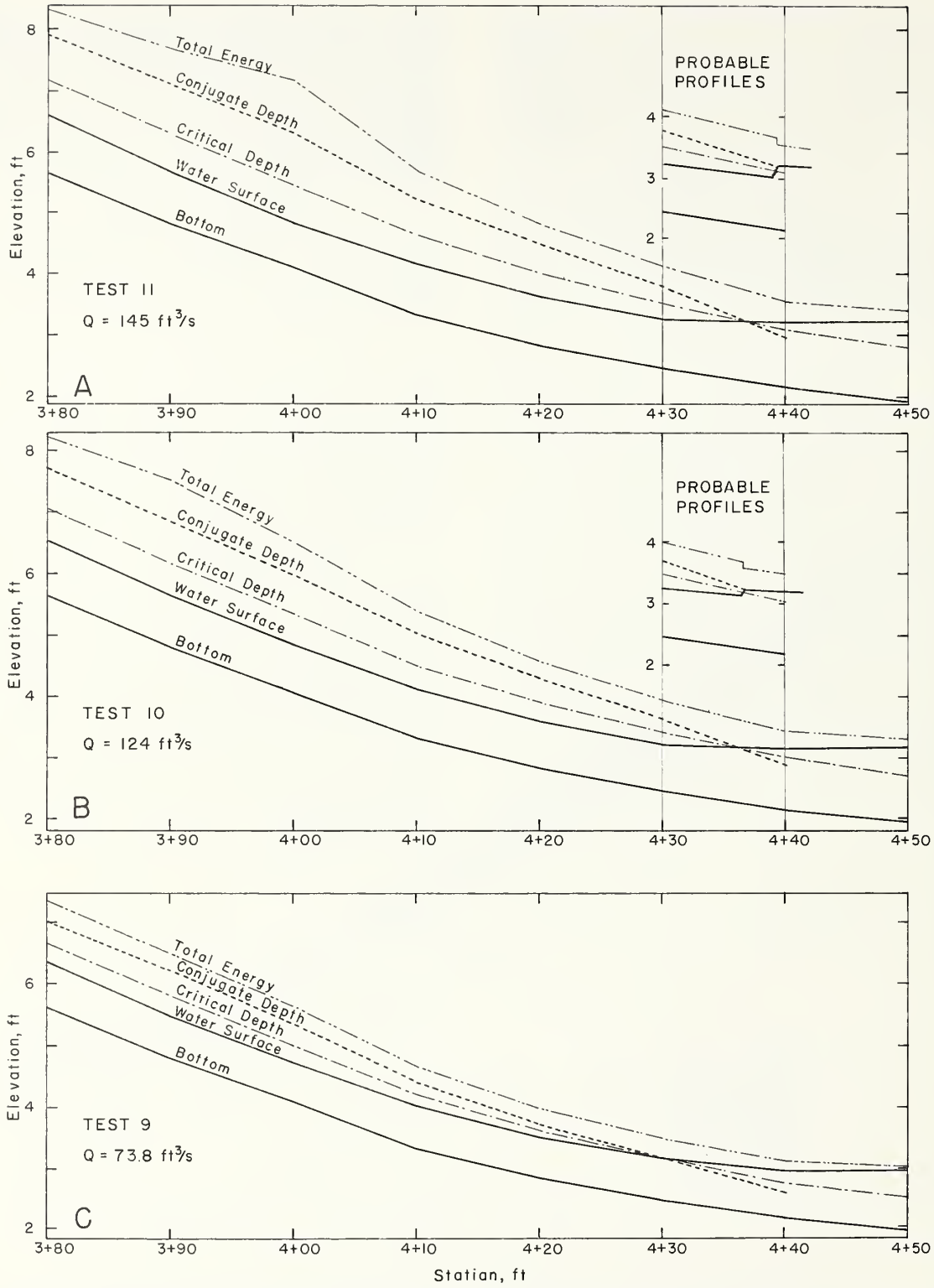

FIGURE 8.—Observed water-surface profiles, calculated hydraulic-characteristic profiles, and estimated probable profiles in transition for tests 9, 10, and 11. *A*, test 11. *B*, test 10. *C*, test 9.

$$n=\frac{1.486}{V}R^{2/3}S^{1/2},$$

where n=Manning n,
V=mean flow velocity in the reach (feet per second),
R=average hydraulic radius (feet),
and S=slope of the energy line (feet per foot).

The mean velocity (V) in a reach was calculated by the relation $V=Q/A$, where Q=discharge rate (cubic feet per second), and A=average area for the reach (square feet).

The average area (A) is the mean of the station areas at the ends of a subreach. The average hydraulic radius (R) is the quotient of the average area and the average wetted perimeter for a subreach. The calculation of the energy-line slope (S) required adding the velocity head—$V_s^2/2g$, where V_s=station velocity (feet per second), and g=acceleration of gravity (feet per second squared)—to the average water-surface elevation at each station to obtain the energy-line elevation. The energy-line drop over a subreach divided by the reach length equals the energy-line slope.

Figure 7 shows the calculated Manning n values plotted against the corresponding values of the product of velocity and hydraulic radius (VR).

Profiles

Various profiles (fig. 8) were plotted for each test to aid in the analysis of the hydraulic performance of the transition. These profiles are of the (1) channel bottom, (2) water surface, (3) total energy, (4) critical depth, and (5) conjugate depth. The plotted elevation of the channel bottom is the average of the elevations of the measured points across the level portion of the channel cross section. The water-surface elevation is the average of the right- and left-edge elevations. The total-energy-line elevation at a station was determined by adding the station velocity head ($V_s^2/2g$) to the water-surface elevation at the station.

The critical-depth elevation was read from

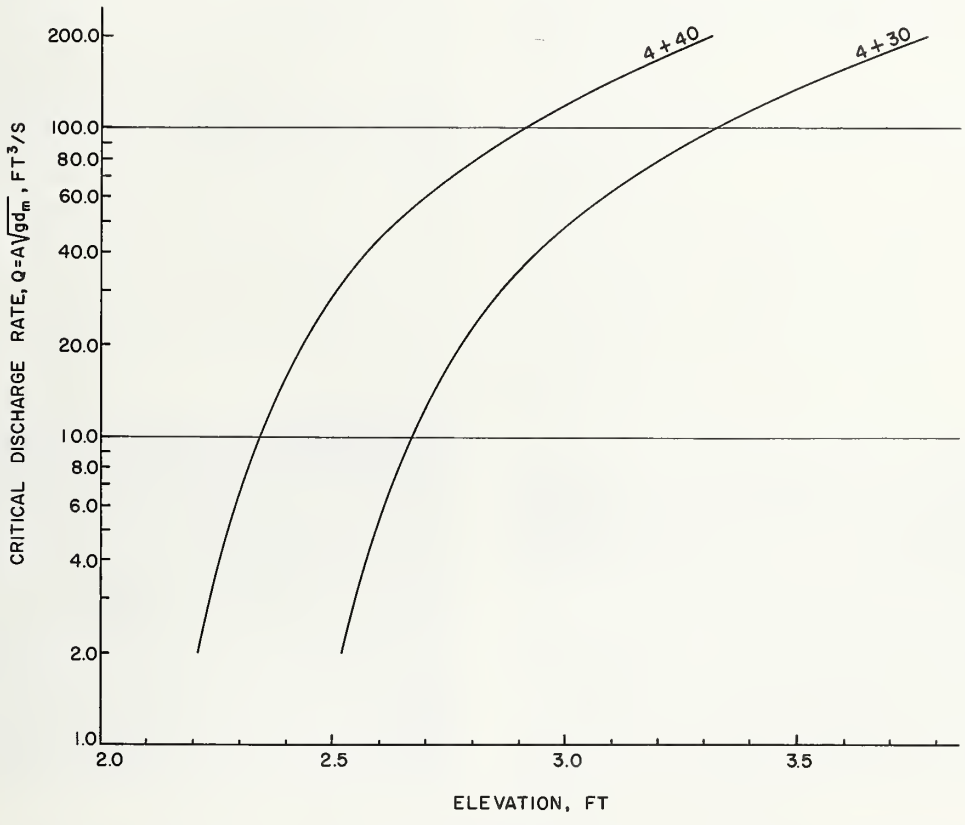

FIGURE 9.—Discharge rate with flow at critical depth versus water-surface elevation at stations 4+30 and 4+40.

a curve (fig. 9) of water-surface elevation versus the function

$$A\sqrt{gd_m},$$

where A=cross-sectional area (square feet),
g=acceleration of gravity (feet per second squared),
and d_m=mean depth, calculated by dividing cross-sectional area by top width, (feet).

At critical flow the discharge rate (Q) is equal to $A\sqrt{gd_m}=A_c\sqrt{gd_c}=A_cV_c$, where the subscript c refers to the critical flow in cubic feet per second. The curve was entered with the discharge rate to read the critical-depth elevation.

The conjugate-depth elevation was calculated with the method presented in H. W. King's "Handbook of Hydraulics,"[3] which states, ". . . for a given discharge in any channel, if water flows at a given depth, there will always be another depth such that the sum of force due to velocity plus hydrostatic pressure at respective cross sections will be the same. If the sum of these forces is designated by the symbol F_m, (*the relationship*) can be expressed in the general form $F_m=Q^2/gA+A\bar{y}$." The definitions of the terms in the equation are: F_m=pressure plus momentum per unit weight of fluid (cubic feet), Q=discharge rate (cubic feet per second), g=acceleration of gravity (feet per second squared), A=cross-sectional area (square feet), and $\bar{y}$=depth to center of gravity of cross-sectional area (feet).

Implicit in this equation is the weight of the fluid. If each term were multiplied by the unit weight of the fluid in pounds per cubic foot, the dimensions of each term would be in pounds. Omitting the fluid unit weight gives each term a dimension of cubic feet, which is not the dimension of a force. Thus, it is not appropriate to apply the term force to identify F_m as King did. However, the equation he presents is in its simplest form and has computational convenience, so it was used in this work. The use of the equation posed one small problem. The computational dimension of F_m was in cubic feet, and to term it a force would have been disturbing, so the more cumbersome identification of pressure plus momentum per unit weight of fluid (simplified to pressure plus momentum) was used.

The curves of pressure plus momentum versus water-surface elevation were plotted for each station for each test; see figure 10 for an example. The elevation of the conjugate depth

[3] McGraw-Hill Book Co. New York, ed. 4, pp. 8–25. (1954).

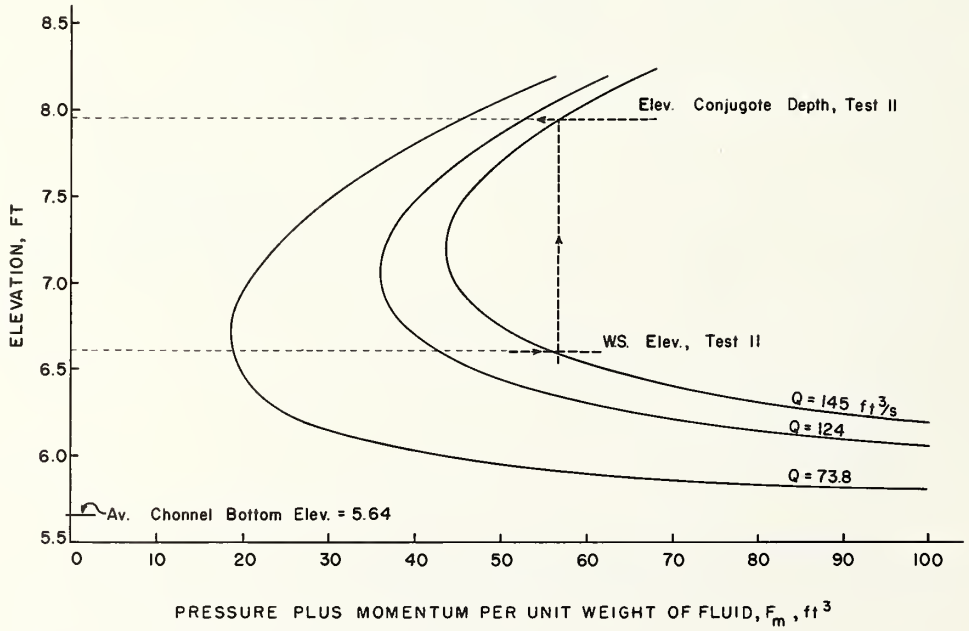

FIGURE 10.—Pressure plus momentum versus water-surface elevation at three discharge rates for station 3+80.

of flow is vertically above or below the point of intersection of the water-surface elevation and the appropriate discharge-rate curve. The pair of conjugate elevations correspond to water-surface elevations before and after a hydraulic jump. The pressure-plus-momentum equation is correct for level channels, but for sloping channels an error is introduced that increases with the $\cos^2$ of the slope angle. In this experiment the slope of the reach in which a hydraulic jump occurred was only 1.5 percent, so the error did not exceed 0.05 percent; thus, the equation is sufficiently accurate.

RESULTS AND DISCUSSION

The observed water-surface profile for test 11 (fig. 8*A*) shows that the flow passed from less than to greater than critical depth between station 4+30 and 4+40. However, the photographs of the flow in the transition show no visible hydraulic jump (figs. 11 and 12). An explanation for this effect is that a jump did occur but was too small to be seen in the turbulent flow. Calculated values of Manning n show that a higher than expected energy loss occurred in subreach 6, between stations 4+30 and 4+40, indicating the presence of a jump in which energy was lost. Because the profiles in this subreach indicate that a hydraulic jump was possible, the water-surface profile could have been like that shown in figure 8*A*. The jump is there, but it is only 0.09 ft high and is too small to be noticed on the water's rough surface.

A similar study of the profile in the same subreach was made for test 10 with a flow of 125 ft^3/s. The profile in figure 8*B* indicates the possibility of a 0.06-ft-high jump. For the next lower flow (test 9 with 73.8 ft^3/s) no evidence of a jump was found (fig. 8*C*). For this flow the transition was probably proportioned correctly to pass the flow through the critical depth without a hydraulic jump.

Manning n Values

The n–VR curves (fig. 7) for the subreaches parallel and lie close to the class C retardance curve, which was the expected curve for the cover in this transition. Also, the figure shows that the curves for subreaches 1 and 2 lie appreciably below the class C curve and that the curves for the other subreaches lie close to, or above, this curve. Two explanations can be found for the relative positions of the n–VR curves. In subreaches 1 and 2, the average stem length of the bermudagrass was 5.3 in, or slightly shorter than the 6-in length of the class C retardance cover. In the subreaches downstream of subreaches 1 and 2 the average grass-stem length was 7.1 in, so larger n values could be expected for these downstream reaches.

Flow deceleration may also explain the larger n values for the downstream subreaches. In subreaches 1 and 2 the flows were nearly uniform or slightly accelerated. In subreaches 3, 4, and 5 the flow slowly decelerated, and in subreaches 6 and 7 the flows rapidly decelerated. Was the deceleration responsible for the increase in n? The question cannot be answered with certainty because the grass-stem length was changing. Also, the change in the n value was small. The most striking feature of figure 7

FIGURE 11.—Flow of 145 ft^3/s in transition, as viewed from upstream, test 11.

FIGURE 12.—Flow of 145 ft^3/s in transition, as viewed from downstream, test 11.

is the departure of the Manning n values from the expected trend for the last three tests on subreach 6. The observed and expected values for n are given in table 2.

A value of n larger than the expected value is believed to be due to the energy loss in a hydraulic jump. This supposition can be tested by calculating the subreach energy loss for the expected n values. If the difference between this calculated loss and the observed loss is equal to the energy loss due to the hydraulic jump, the supposition is probably valid. Test 11 was used in this calculation, with the water-surface profile shown in the inset of figure 8*A*.

New values of A, P (wetted perimeter), R, and V were calculated. In calculating these new values it was assumed that no jump had occurred in the subreach. The water-surface elevation at station 4+40 was estimated. The cross-sectional area at station 4+40 for the estimated water-surface elevation was averaged with the cross-sectional area at station 4+30 to obtain the new average for A. The wetted perimeter was treated in a like manner. The expected value of 0.042 was chosen for n. With the new values, the slope of the energy line was calculated from the Manning formula.

$$S=\frac{V^2n^2}{2.208\,R^{4/3}}=\frac{6.54^2\times0.042^2}{2.208\times0.743^{4/3}}=0.051.$$

Thus, the energy loss for the 10-ft subreach was $10\times0.051=0.51$ ft.

The estimated energy loss due to friction alone was probably slightly large because downstream of a jump the higher water surface (WS) would have yielded a lower velocity and a smaller head loss. However, the calculated location of the jump was station 4+39, leaving only 1 ft of channel at a velocity lower than that used in the calculation. The error is small, and the approximation of the head loss is acceptable. The actual energy loss in the subreach was 0.605 ft, or 0.095 ft larger than that calculated for the 10-ft subreach. The energy loss in the hypothesized hydraulic jump (H_j), as estimated by the Bernoulli relationship, is

$$\Delta H_j=(WS\text{ elev. }1+\frac{V_1^2}{2g})-(WS\text{ elev. }2+\frac{V_2^2}{2g})$$

$$\Delta H_j=(3.08+0.624)-(3.24+0.620)$$

$$\Delta H_j=0.156\text{ ft.}$$

The agreement between the two estimated energy-loss calculations (0.095 ft and 0.156 ft) is not as close as was hoped for. However, they are not so different as to positively invalidate the proof of the supposition than an increase in the n value indicates the presence of a hydraulic jump.

TABLE 2.—*Observed and expected values of Manning* n *for subreach 6*

Test No.	Discharge rate (ft^3/s)	VR value (ft^2/s)	Manning n values	
			Observed	Expected
9	73.8	2.53	0.058	0.053
10	124	4.09	.056	.044
11	145	4.74	.057	.042

Transition Performance

The transition, which performed admirably, suffered neither erosion nor loss of cover from the test flows. No change can be detected in

TABLE 3.—*Cross-sectional data, flow depths and velocities, Froude numbers, wave angles, and wall-divergence angles for transition during test 11*[1]

Station	Area (ft^2)	Top width (ft)	Hydraulic depth (ft)	Velocity (ft/s)	Froude No.	Wave angle (degrees)	Wall-divergence angle	
							Right (degrees)	Left (degrees)
3+80	13.91	16.95	0.82	10.4	2.03	29.6	0	0
3+90	12.36	17.25	.72	11.7	2.44	24.2	1.8	2.8
4+00	11.76	18.82	.62	12.3	2.75	21.4	3.6	5.6
4+10	14.58	21.56	.68	10.0	2.13	28.0	5.4	8.3
4+20	16.47	23.55	.70	8.80	1.85	32.6	7.2	11.0
4+30	19.26	26.70	.72	7.53	1.56	39.8	8.9	13.7
4+40	31.78	33.95	.94	4.56	.83	...	10.7	16.3

[1] Flow of 145 ft^3/s.

FIGURE 13.—Transition after tests, as viewed from upstream.

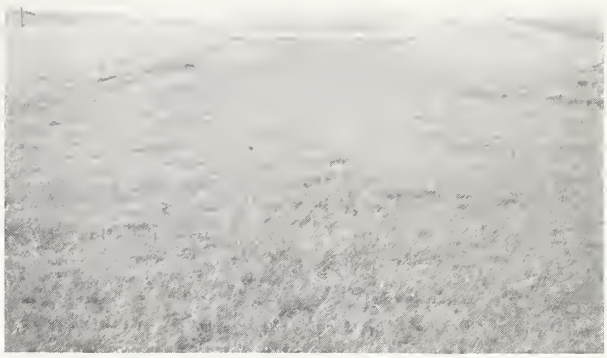

FIGURE 14.—Transition after tests, as viewed from downstream.

the before (figs. 4 and 5) and after (figs. 13 and 14) appearances of the transition. The good performance of the transition is attributed to the gradual convergence of the conjugate depths. The hydraulic jump, if present at all, was small. This result was accomplished by widening the channel cross section and by reducing the bed slope in the downstream direction, a combination that caused the flow depth to remain relatively constant in the transition section and the flow velocity to gradually decrease.

The angle of divergence of the channel sides was less than the wave angle at all stations. According to Woodward and Posey[1] this limitation of the divergence rate is a requirement to avoid standing waves. Wave angles and divergence angles for the transition during test 11 are given in table 3, along with velocity and flow-depth data.

The mean flow velocity in the transition section reached a maximum of 12.32 ft/s, which is considerably in excess of the 8 ft/s suggested in the "Handbook of Channel Design for Soil and Water Conservation" (see footnote 2) as a permissible velocity for the soil and cover at this site. However, in the laboratory, where channel smoothness and excellent grass can be maintained, the data show that the design velocity can be exceeded. Channels in the field are seldom as uniform and smooth surfaced as those in the laboratory nor is the grass cover as well maintained, so permissible velocities lower than those in the laboratory are recommended.

CONCLUSIONS

The excellent performance of the channel transition in bringing supercritical velocity flows onto a flat-bottom area without damage to the bermudagrass lining is attributed to the following:

1. Careful shaping of the transition so that changes in width and bottom slope were smooth and gradual.
2. Maintaining a dense, uniform bermudagrass cover.
3. Widening the transition to reduce flow velocity.
4. Reducing bed slope so depth was unchanged as the channel was widened.
5. Changing the width and slope to bring the conjugate depths close together before a hydraulic jump could form, or so the jump, if present, would be small and nondestructive.
6. Keeping the divergence angle of the channel sides smaller than the wave angle of the supercritical velocity flow.

[1] Woodward, S. M., and Posey, C. J. 1941. Hydraulics of steady flow in open channels, p. 124. John Wiley & Sons, Inc., New York.

* 1977-GPO-1750-S/771-040/11

U. S. DEPARTMENT OF AGRICULTURE
AGRICULTURAL RESEARCH SERVICE
SOUTHERN REGION
P. O. BOX 53326
NEW ORLEANS, LOUISIANA 70153

OFFICIAL BUSINESS
PENALTY FOR PRIVATE USE, $300

POSTAGE AND FEES PAID
U. S. DEPARTMENT OF
AGRICULTURE
AGR 101